International Journal of Adhesion & Adhesives 129 (2024) 103600

Contents lists available at ScienceDirect

International Journal of Adhesion and Adhesives

journal homepage: www.elsevier.com/locate/ijadhadh

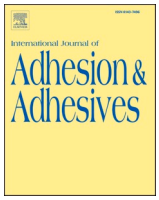

Influence of high frequency on the fatigue life of metallic single lap joints

F. Moroni *, F. Musiari, A. Pirondi

Università di Parma, Department of Engineering and Architecture, Parma, Parco Area Delle Scienze 181/A, 43124, Italy

ARTICLE INFO

Keywords:
C. Fatigue
A. Epoxides
B. Metals
High frequency fatigue testing

ABSTRACT

Polymer adhesives are known to exhibit time dependent mechanical behaviour, that becomes more and more evident approaching the glass transition temperature, T_g. When subjected to fatigue, bonded joint lifetime can be therefore affected by the loading frequency and amplitude. According to the literature, the influence of the frequency on the fatigue behavior manifests as a rise of the temperature in the adhesive due to the hysteretic heating, which is related in turn to T_g and to the viscoelastic properties of the adhesive. In this paper, cyclic loading was applied to single lap shear joints until failure at frequencies in the range of 70–90 Hz, that are little explored by the existing literature. The aim is twofold: on one side, to investigate the possibility to speed up fatigue tests in comparison to tests performed in the range of 7–9 Hz; on the other side, to explore the possibility to generate stress-life data in a range of number of cycles between 10^6 and 10^8, therefore two order of magnitude higher then usual, without exceeding with the time required for the tests. The joints were made with both aluminum and stainless-steel substrates bonded with a structural epoxy adhesive, to manufacture a Single Lap Joint (SLJ). Two loading ratios R (respectively 0.1 and 0.4, defined as the minimum over the maximum force of the fatigue cycle) and different load ranges were applied. Digital Image Correlation (DIC) technique was used to assess the presence of creep strains. A preliminary investigation consisting in a Dynamic Mechanical Analysis (DMA) of bulk adhesive for the range of frequency of interest, and in the measurement of the temperature of the adhesive layer during some selected fatigue tests was carried out. No significant changes of the viscoelastic properties of the adhesive were found for the frequency of interest, and, at the same time, temperature measurements revealed that the temperature increased by a few degrees, remaining in any case far from the glass transition temperature. The test results showed that only small effect due to the application of a high frequency cyclic loading on the fatigue life apparently occurs for tests carried out at the lowest load ratio, in particular when the applied loads were relatively low, and the number of cycles at failure relatively high. On the opposite, the results of tests carried out at the highest load ratio are affected by the loading frequency, and it has been related to the presence of significant creep deformation within the adhesive layer.

1. Introduction

Adhesive bonding has become quite a popular joining technique, especially for lightweight structures, since it enables several advantages over fastening or welding (e.g. light weight, possibility to join dissimilar materials, sealing, …). From the mechanical standpoint, it offers also longer fatigue life than conventional joining techniques [1]. However, under fatigue loading, also adhesive joints may fail at a small fraction of static strength. Therefore, an accurate prediction of fatigue life is mandatory and this requires first of all to have reliable stress-life data. Fatigue testing of adhesive joints is a consolidated activity [1], which even in the recent past offered several insights related to the influence of environmental conditions (i.e.: temperature and moisture) [2–4], behavior of hybrid [5] or multi-material joints [6,7] effectiveness of reinforcements [8], predictive models [9,10] and other inherent topics [11–13]. Fatigue testing is typically performed at low frequencies (1–10 Hz) in order to avoid hysteretic heating of the adhesive. For example, in Ref. [14] the authors stated that a too slow frequency would yield an extremely long testing time; on the other hand, a too high frequency would introduce the heating of the joint due to adhesive hysteresis. With the help of a thermographic camera, they found a good balance by working at 12 Hz.

Since adhesive joints are inherently multi-material, and several additional factors have an effect on the fatigue strength, such as mean stress, presence of an adhesive fillet or chamfer, temperature, etc., the reduction of testing time is of significant importance to investigate the

* Corresponding author.
E-mail address: fabrizio.moroni@unipr.it (F. Moroni).

https://doi.org/10.1016/j.ijadhadh.2023.103600
Received 31 July 2023; Received in revised form 7 October 2023; Accepted 10 December 2023
Available online 14 December 2023

Table 1
Mechanical properties of the materials used for the adherends manufacturing (taken from supplier certificate).

Material	AA6082-T6 (AL)	AISI 304 (SS)
Young modulus, E_s	70 GPa	190 GPa
Poisson's ratio, ν_s	0.33	0.29
Tensile yield strength, Rp_s	295 MPa	230 MPa
Tensile ultimate strength, Ru_s	320 MPa	510 MPa

Table 2
Mechanical properties of Loctite Hysol 9466 (taken from datasheet available on www.henkel.com).

Material	Loctite Hysol 9466
Young modulus, E_a	1718 MPa
Tensile ultimate strength, Ru_a	32 MPa
Glass transition temperature, Tg	62 °C

effect of such factors on the fatigue strength [15]. On the other hand, several components are subjected to cyclic loading at a frequency well above those typically tested in lab, meaning that high frequency testing would contribute to release stress-life data closer to the operating conditions.

The influence of different frequency rates on bond durability of self-etch adhesives to enamel was studied in Ref. [16] at frequencies of 5Hz, 10Hz, and 20 Hz, recording similar fatigue strength.

Xu et al. [17] tested fatigue crack growth on filled and toughened steel adhesive joints in the range 0.02–20 Hz in steps of a decade, finding that the fatigue crack growth rate increases as frequency decreases. They postulated that this occurs due to the decrease of strength with decreasing frequency which, in turn, causes a wider crack tip process zone. Similar conditions and findings are present in Ref. [18].

Constant and variable amplitude fatigue loading was tested in Ref. [19]. In order to evaluate if the adhesive under test was prone to hysteretic heating, the temperature was monitored by two thermocouples embedded into the adhesive layer. The results demonstrated that up to the maximum frequency evaluated (30 Hz) there was no appreciable increment of temperature.

A thermal camera was used in Ref. [20] to monitor the surface temperature of fatigue loaded specimens to detect heating due to high frequency, where high frequency was set as 25 or 40 Hz for comparison with the 10 Hz baseline. They found that the slope of the stress-life best-fit increased for an increasing frequency, although all data seems to fall within a unique scatter band.

The studies of [21] were done on stainless steel Single-Lap Joint (SLJ) bonded with an electrically conductive adhesive. Loading in the range 50–150 Hz revealed that the influence of the frequency on the fatigue behavior depends on the rise of temperature in the adhesive due to the hysteretic heating, the glass transition temperature and the viscoelastic properties of the adhesive.

Trapezon [15] and Tridello [22] used ultrasonic (US) frequencies (10 KhZ and 20 KHz, respectively) to speed up testing, by developing a custom bonded specimen for the ultrasonic testing device. In particular, in Ref. [22] it was shown that by limiting the temperature to 22 °C near the joint using two vortex tubes conveying a cold air flux towards the bondline, it was possible to keep the temperature inside the adhesive almost constant, and keeping the increment during the test to within 9 % of the initial value. However, besides the need of cooling the specimen, a drawback of US testing is that the specimen has to be specifically developed for the materials under test to fit to the dynamics of the test system.

The effect of hold time between fatigue cycles was evaluated in Ref. [23] using double butt-strap specimens of glass and polycarbonate bonded with an acrylic adhesive. A very remarkable decrease of fatigue life was found by increasing the hold time at maximum load, P_{MAX}, while no effects were noticed for a hold time at minimum load, P_{MIN}. A decrease of lifetime was also found for an increasing load ratio ($R = P_{MIN}/P_{MAX}$), indicating the importance of creep on fatigue lifetime.

From the previous literature analysis, it is quite clear that the influence of frequency on fatigue strength of adhesive joints is still far from being well-encased. In particular, a systematic increase in temperature with increasing frequency is not found, except at US frequencies, were cooling is clearly necessary but, despite this, high-frequency testing is little explored with a few exceptions ([15,21,22]). Besides, in some adhesives the creep-fatigue interaction may be overwhelming, as shown in Ref. [23].

Therefore, the aim of this paper is to investigate the suitability of high frequency testing for the characterization of epoxy adhesively bonded joints. This will result in a quite unexplored detection of the possible advantages and drawbacks of a such kind of tests, specifically aimed at identifying their field of feasibility with respect to the topic represented by the fatigue behavior of joints. Therefore, the possibility to exploit high frequency tests for fatigue characterization would enable two types of consequences, both linked to the reduction of the time for testing and quite untouched by existing literature: the possibility to speed-up tests for the same ranges of cycles to failure usually investigated with low frequency tests and also the possibility to generate stress-life data in a range of cycles to failure between 10^6 and 10^8, i.e. two order of magnitude higher than the previously mentioned ones, without exceeding with the time usually required for testing. Experimental tests were carried out on aluminum and stainless steel single lap joints, with loading frequency ranging between 70 and 90 Hz using a resonance testing machine. The results of these tests were compared with other carried out with frequency in the range 7–9 Hz. Two different loading ratios ($R = 0.1$ and 0.4) were applied to look for the effect of a different mean stress on lifetime. Digital Image Correlation (DIC) technique was used to monitor the displacement on one side of the joint during the test development. Preliminary investigation consisting in Dynamic Mechanical Analysis (DMA) and in measurements of temperature within the bonded area during the test, were performed, in order to exclude any possible influence of the hysteretic heating on high frequency mechanical tests.

2. Experimental setup

2.1. Materials and geometry

Two different materials were selected for the adherends manufacturing, specifically an aluminum alloy (AL - AA6082-T6) and a stainless steel (SS - AISI 304), both supplied by Bernazzoli srl (Parma, Italy), whose properties are listed in Table 1. The adhesive was a toughened two-part epoxy (Loctite Hysol 9466, Henkel Italia, Milano, Italy), whose nominal properties are illustrated in Table 2.

The Single Lap Joint was chosen as test geometry. The main dimensions of the specimens are provided in Fig. 1 and Table 3. The geometry was selected in accordance with ASTM D 3166 [24] with some changes concerning overlap length and substrate thickness in order to avoid the fatigue breakage of substrates possibly induced by the tensile stresses generated by the bending of the substrates in the proximity of the end of the overlap length, especially in the case of aluminum specimens.

2.2. Joint preparation

The adherends were firstly cleaned to remove any contaminant possibly coming from the machining step. Then, a grit blasting pre-treatment was applied on the surface in order to increase its roughness and wettability. The procedure employed alumina particles (grade 80) and was performed at a pressure of 0.5 MPa, with a distance of 30 mm from the nozzle and the treated surface, for a time of approximately 1 min per substrate to cover the entire area of the overlap. In order to

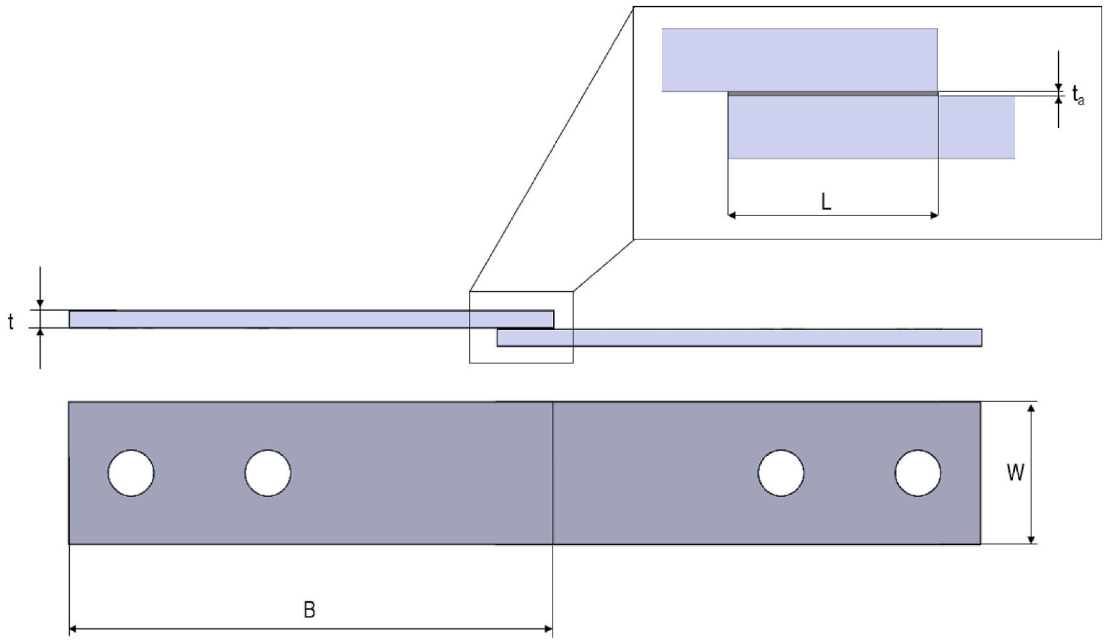

Fig. 1. SLJ geometry.

Table 3
SLJ dimensions.

L (mm)	ta (mm)	t (mm)	B (mm)	W (mm)
10	0.20	3	85	25

Table 4
Average values and standard deviations of surface roughness (Sa) before and after grit blasting.

Substrate Material	Sa [μm]	
	Before Grit Blasting	After Grit Blasting
Aluminum	0.42 ± 0.10	3.10 ± 0.49
Stainless Steel	0.68 ± 0.06	1.83 ± 0.23

prove the effectiveness of the treatment, the surface roughness (Sa) of the specimens was measured before and after grit blasting, using a CCI MP-L (Taylor Hobson, Leicester, UK) digital optical profilometer following ISO 25178 [25]. Five measurements were performed for every surface condition: the average values and standard deviations are given in Table 4.

After the grit-blasting, the surfaces of the adherend were rinsed with water and cleaned with Henkel 7063 chemical degreaser just before the adhesive deposition. The adherends were finally bonded together: the correct values of overlap length and adhesive thickness, as such as the correct alignment of the substrates, were ensured by following the procedure described in Ref. [26]. The adherends were provided with two drilled lateral flanges, where two small bolts were fastened to hold together the parts during the adhesive curing. The thickness of the adhesive, t_a, set to 0.2 mm, was controlled by means of calibrated metal washers. At the end of the assembly procedure, the excess of the adhesive was accurately removed from each end of the overlap length using a specifically designed spatula, with the aim of obtaining a square fillet. However due to the adhesive viscosity the fillet assumed a rounded shape, with a radius in the range between 0.2 and 0.4 mm, as for example shown in Fig. 2. The cure of the joints was performed in a controlled climatic chamber, at 80 °C for 60 min, consistently with the

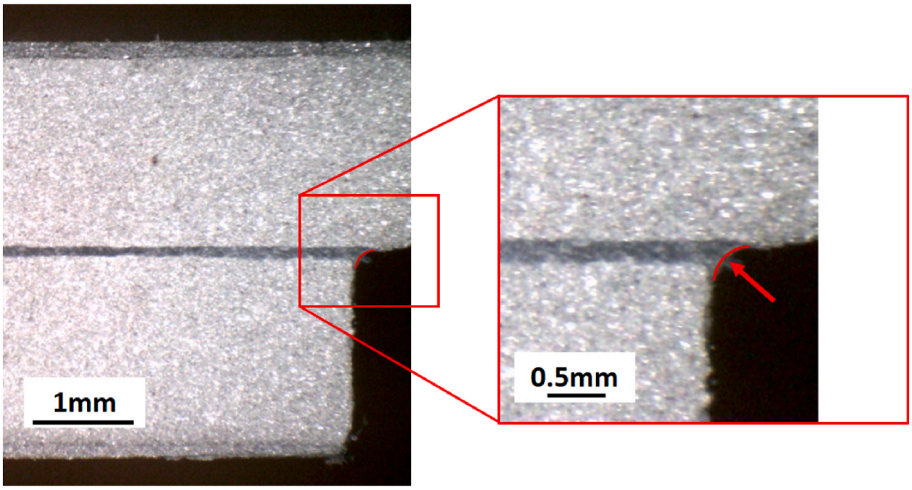

Fig. 2. Detail of the shape of the fillet.

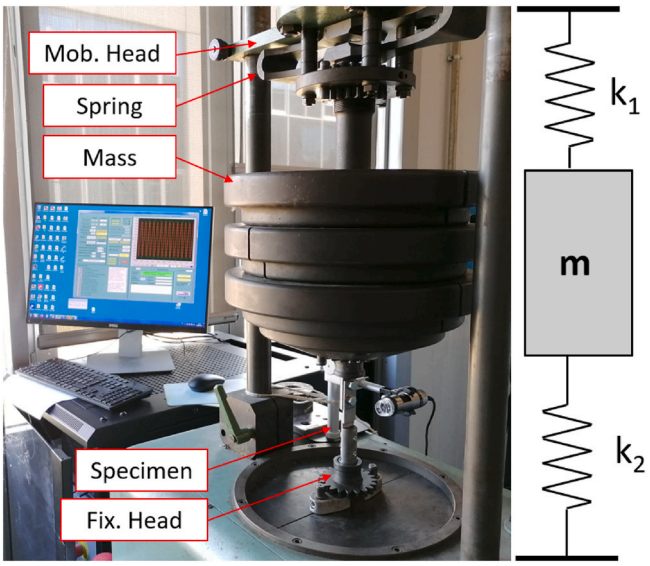

Fig. 3. Amsler HFP 422 high-frequency pulsator and its schematic representation as a vibrating system.

Table 5
Fatigue test frequencies.

Substrate Material	Aluminum (AL)	Stainless Steel (SS)
Low Frequency (LF)	7 Hz	9 Hz
High Frequency (HF)	70–73 Hz	88–90 Hz

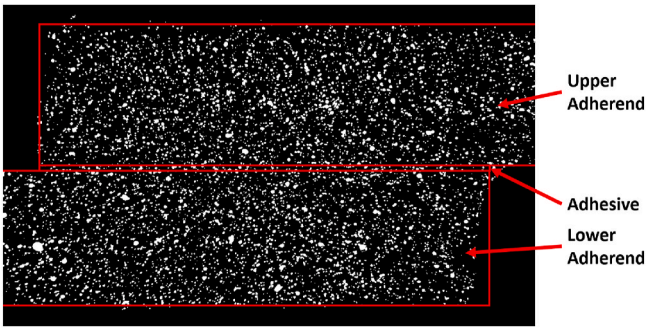

Fig. 4. Example of images captured for DIC (side view of the overlap).

supplier indications. Once the curing was completed the two flanges were cut away to allow the testing of the specimens.

2.3. Fatigue mechanical characterization

The tests required the application of a sinusoidal wave-shaped load cycle. The cycle was characterized by a maximum and minimum load (P_{MAX} and P_{MIN} respectively). By the knowledge of the latter also the average cyclic load P_M, the load amplitude P_A and the load ratio R, can

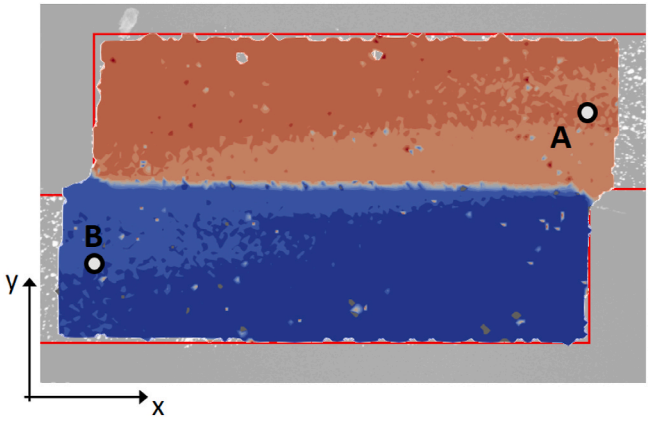

Fig. 6. Example of result of Digital Image Correlation (displacement along x direction).

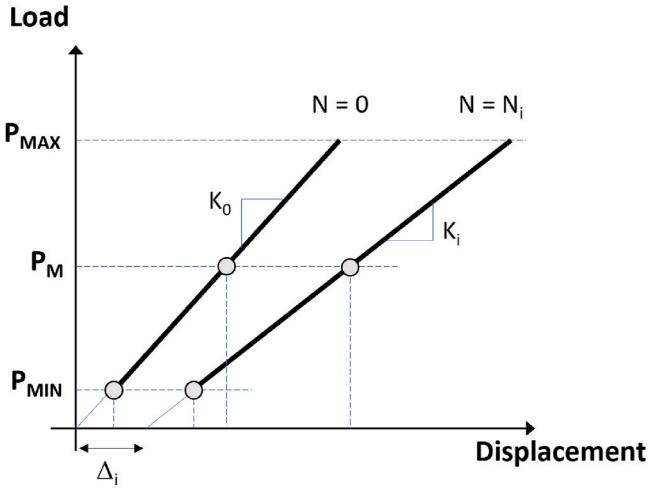

Fig. 7. Example of change of load curve during a fatigue test.

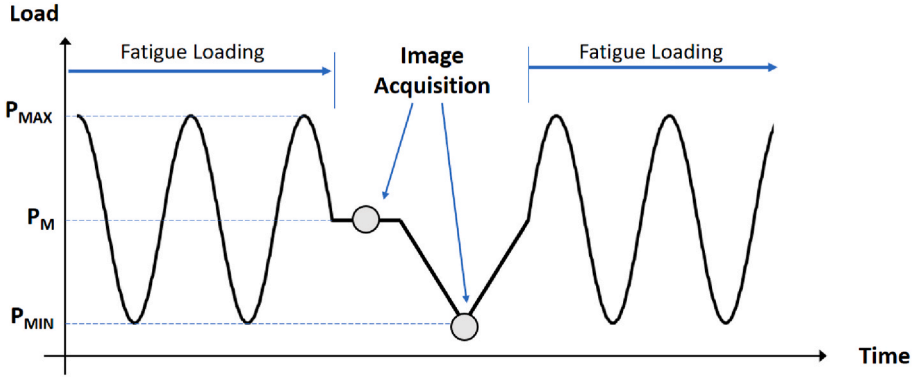

Fig. 5. Schematic representation of the sequence for the image acquisition.

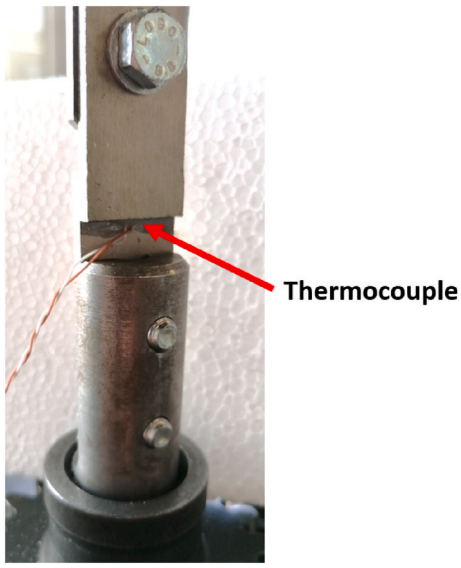

Fig. 8. Location of the thermocouple embedded in the adhesive layer.

be defined as follow:

$$P_M = \frac{P_{MAX} + P_{MIN}}{2} \quad (1)$$

$$P_A = \frac{P_{MAX} - P_{MIN}}{2} \quad (2)$$

$$R = \frac{P_{MIN}}{P_{MAX}} \quad (3)$$

Knowing the average cyclic load (P_M) and the load amplitude (P_A), along with the length (L) and the width (W) of the overlap, the cyclic average shear stress (τ_M) and the cyclic shear stress amplitude values (τ_A) can be defined as follow:

$$\tau_M = \frac{P_M}{LW} \quad (4)$$

$$\tau_A = \frac{P_A}{LW} \quad (5)$$

In this work two different load ratios were explored for both the materials, R = 0.1 and R = 0.4. The first one is the load ratio suggested by the ASTM D 3166, while the second was specifically selected to investigate the effect of higher average load on the fatigue behaviour of joints tested with different loading frequency.

The data resulting from the tests were analyzed using a stress-life approach, and therefore the fatigue curve was obtained by plotting the cyclic shear stress amplitude τ_A during a cycle versus the number of cycles to failure, N_f, assuming a log-normal distribution of N_f according to Eq. (6):

$$\tau_A = kN_f^{\mu} \quad (6)$$

where k is the intercept of the curve for $N_f = 1$, and μ is the slope of the curve in a double logarithmic graph $\tau_A - N_f$.

The high-frequency fatigue tests were performed in an Amsler HFP 422 high-frequency pulsator with a static load range of 20 kN and a dynamic load range of ±10 kN. The machine (Fig. 3) consists of a fixed and a mobile head, which allows for applying a static load, in this case set to the mean load of the applied cycle. Then, an electromagnetic drive produces the oscillation at the resonance frequency of the load chain (composed by the stiffness k_2 of the specimen, the mass m, and a spring of stiffness k_1), in order to apply the alternating load. The higher the stiffness of the specimen, the higher the test frequency and, once set the mass, the frequency is fixed during the test. Small changes in a range of a few Hz are possible as a consequence of the increase in compliance related to the damage development in the specimen.

The low frequency tests were performed in a MTS 810 servo-hydraulic machine (MTS, Eden Prairie, USA) equipped with a 100 kN load cell, under load control. With this kind of machine, the test frequency can be controlled and changed, however, it is not suitable to perform fatigue test with a load frequency higher than 15 Hz. In order to emphasize the effect of the test frequency on the fatigue performance of bonded joints, a difference of one order of magnitude was set between High Frequency (HF) and Low Frequency (LF) fatigue test as illustrated in Table 5.

2.4. Fatigue test monitoring

In order to monitor the failure development of the bonded joints during the fatigue tests, pictures of one side of the specimens were taken during the whole test. Moreover, a limited number of specimens were also monitored through the Digital Image Correlation (DIC) technique. Specifically, at regular intervals of time, the fatigue tests were stopped and pictures of one side of the specimen, previously painted with a black

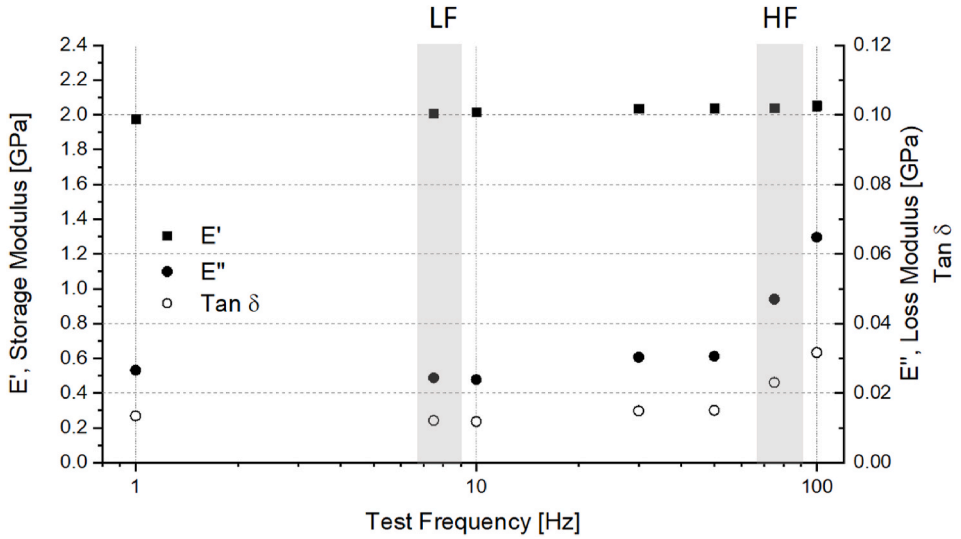

Fig. 9. Result of the DMA on bulk adhesive specimen.

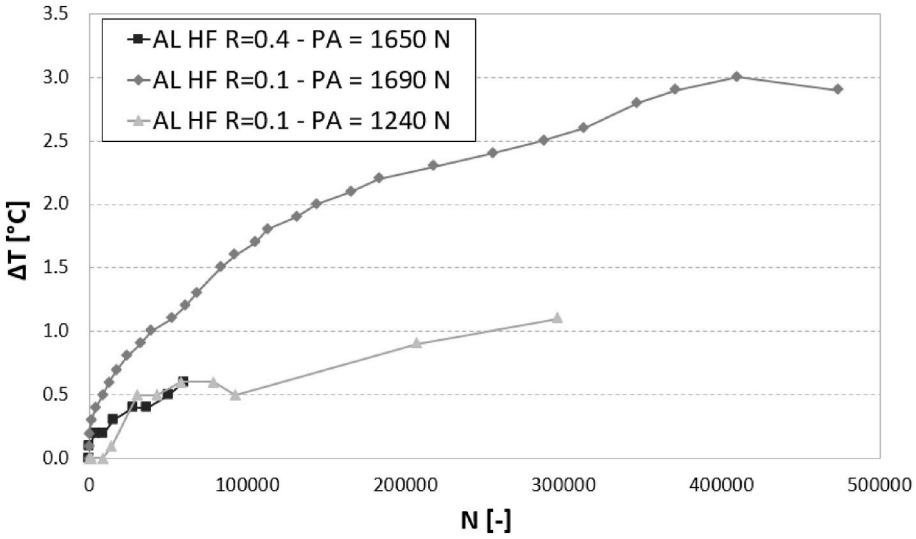

Fig. 10. Measured increase of temperature, ΔT, with respect to initial temperature T0, vs. number of cycles N, for aluminum joints.

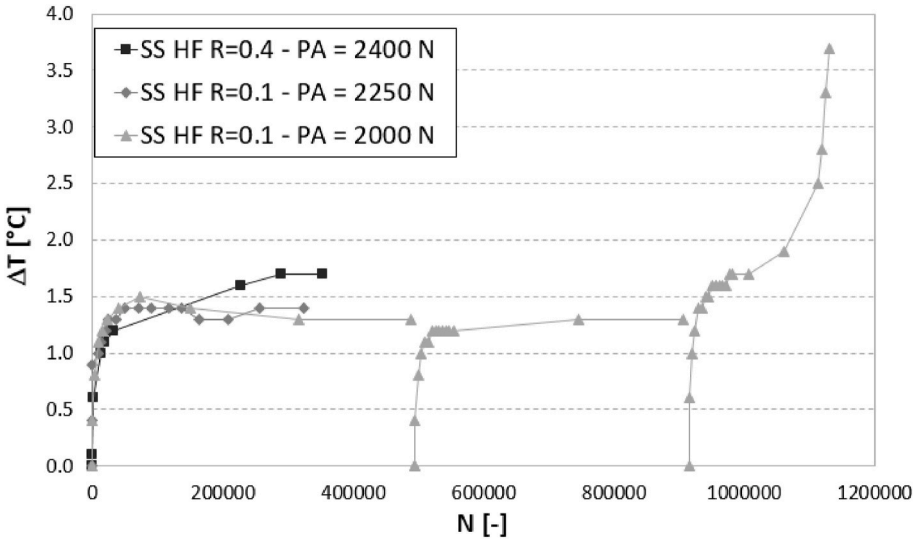

Fig. 11. Measured increase of temperature, ΔT, with respect to initial temperature T0, vs. number of cycles N, for stainless steel joints.

background and white speckles, were captured under a constant static load, by using a 5 MPx Dinolite digital camera (Fig. 4).

The images captured were processed with DICe open-source software [27], in order to obtain the relative displacement of one substrate with respect to the other during the test execution. Correlation results were then post-processed using Paraview [28].

The image acquisitions were performed as schematically shown in Fig. 5: i) fatigue loading was stopped; ii) a load equal to P_M was applied to the specimen; iii) the first image was acquired; iv) a load equal to P_{MIN} was applied to the specimen; v) the second image was acquired; vi) the load was set equal to P_M again, and the fatigue loading restarted.

For each test, to obtain the relative displacement of the two adherends, two points, namely A and B, located in the middle of the substrate thickness, respectively above and below the ends of the overlap (see Fig. 6), were identified in the first undeformed picture. Their positions, and therefore the relative displacement of the adherends, were monitored throughout the entire fatigue test for every acquired image (at P_M and P_{MIN}) using the DIC output.

The knowledge of the displacement at two levels of load (P_M and P_{MIN}) allowed to monitor the mechanical behaviour of the joint along the entire test. Specifically, by interpolating with a linear equation passing through the two points, it was possible to obtain the stiffness (K) and the accumulated displacement (Δ) for each acquisition (see Fig. 7). In particular, the latter could be considered representative of creep deformation of the adhesive layer, since it corresponds to the amount of displacement shown by the joints when the applied load would be zero.

In addition to monitoring the tests during their execution, the fracture surfaces of the failed joints were also analyzed in order to study the failure process. For this purpose, pictures of the fracture surfaces of the two adherends for each joints were taken, again using a 5 MPx Dinolite digital camera.

2.5. *Preliminary investigation*

Before performing the entire experimental campaign, some preliminary tests were carried out in order to determine whether the high frequency fatigue testing of bonded joints would be affected by hysteretic heating due to the viscoelastic properties of the adhesive. For this purpose, Dynamic Mechanical Analyses were performed using a DMA Q800 (TA Instruments, New Castle, DE, USA). In particular, the tests were carried out on 35 mm (length) x 10 mm (width) x 3 mm (thickness) bulk adhesive specimens, tested using a dual cantilever bending

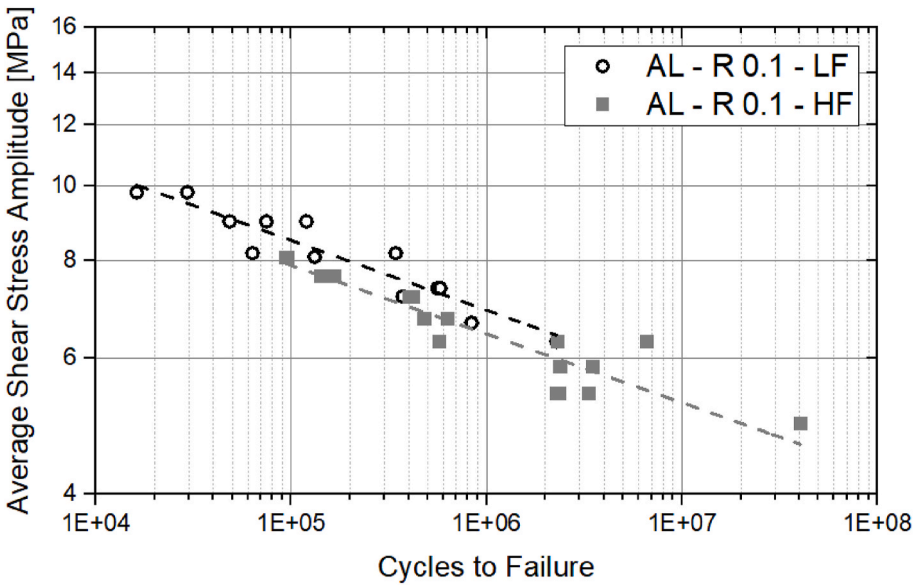

Fig. 12. Result of fatigue test, aluminum specimens, R = 0.1.

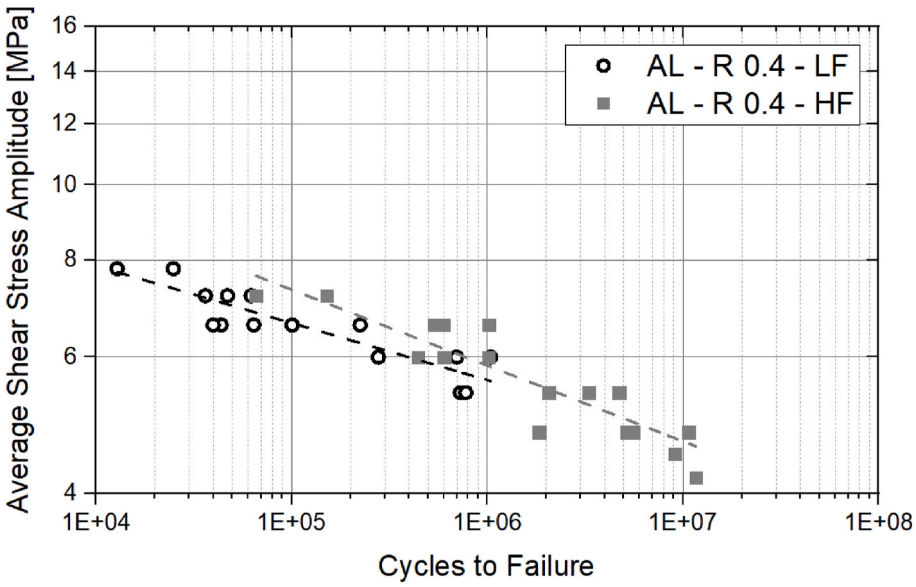

Fig. 13. Result of fatigue test, aluminum specimens, R = 0.4.

configuration. Tests were performed at 25 °C, applying a 0.2 % strain amplitude with testing frequency ranging between 1 and 100 Hz.

Furthermore, for a limited number of specimens, thermocouples were embedded within the adhesive layer to monitor the temperature increase, ΔT, with respect to the temperature at the beginning of the test, T_0, during the high frequency fatigue tests. K-Type thermocouples (Digilent, Inc, Washington, USA) were used: their size was approximately 1 mm × 1.5 mm x 0.2 mm (thickness, the same as the adhesive layer), and they were placed, before curing, within the adhesive layer near the end of the overlap length, where the maximum stress is expected (see Fig. 8). The tests carried out with thermocouples were not included in the following analysis, since they represented a sort of notch that significantly affected the fatigue life of the joint.

3. Results and discussion

3.1. Preliminary investigation

The results of the DMA on bulk adhesive specimens are shown in Fig. 9. The two grey bands highlight the frequency ranges at which the low frequency (LF) and high frequency (HF) tests were performed. It is quite clear that the storage modulus (E′) appeared almost stable over the entire frequency range. On the opposite, the Loss Modulus (E″), and, as a consequence, also tan(δ) remained almost constant in a range of frequencies between 1 and 50 Hz, while they showed a significant increase above the latter value. However, both, E″ and tan(δ) were found to be relatively low, meaning that the behaviour of the adhesive, for the entire frequency range, remained substantially elastic.

Concerning the temperature acquisition during the fatigue test, Figs. 10 and 11 show the increase of temperature ΔT with respect to the initial temperature T_0, plotted against the number of cycles N undergone

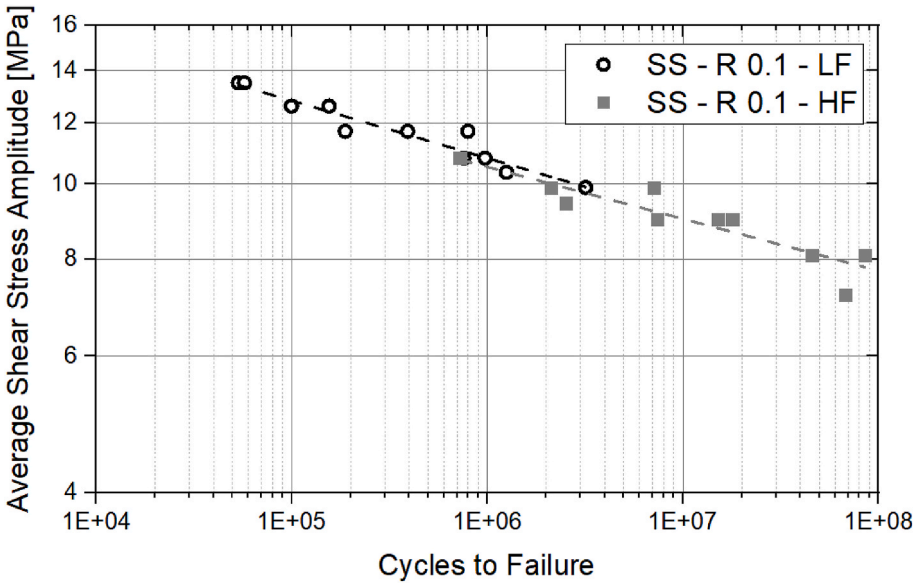

Fig. 14. Result of fatigue test, Stainless Steel specimens, R = 0.1.

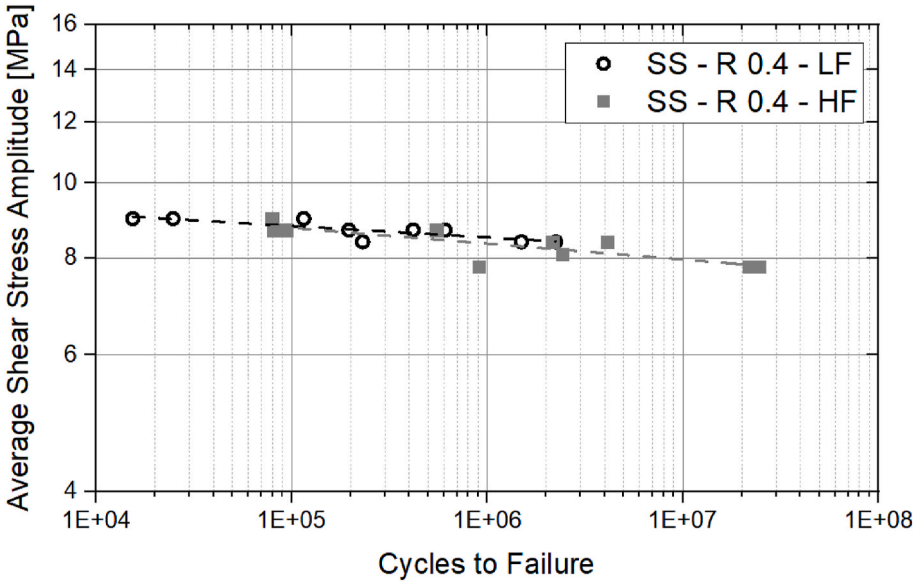

Fig. 15. Result of fatigue test, stainless steel specimens, R = 0.4.

by the specimen, for a selected number of specimens, respectively for both aluminum and stainless steel joints. For both materials considered, measurements showed a fast increase of the temperature at the beginning of the test. The further the test proceeded, the smaller the temperature increase became, until it showed a flat trend, corresponding to a temperature increase, ΔT, limited to 1.5 ÷ 3 °C. This means that the fatigue loading produced localized heating, but the amount of energy dissipated was not enough to significantly increase the temperature of the adhesive, and in any case the latter remained considerably away from the glass transition temperature of the adhesive (Tg, 62 °C).

The only exception to the described trend was the curve obtained by the specimen SS HF R = 0.1 – P_A = 2000 N. This test was stopped and restarted a couple of times, and it can be noticed that the described trend was repeated for every restart, but a few cycles before the complete failure the curve exhibited a further trend consisting in a sudden and fast increase. Since this behavior occurred in the final stage of the joint life, when the crack propagated in the overlap, it could be associated with the occurrence of friction between the adherends due to the possibility of slight sliding of one adherend with respect to the other, enabled by crack propagation. Thus, even in this case, the maximum temperature increase was lower than 4 °C, starting from a value of T_0 approximately equal to 25 °C. Therefore, generally speaking, the trends inferred from the curves, for both the aluminum and the stainless steel joints, allowed to conclude that the effect of the hysteretic heating induced by the high-frequency fatigue load cycles was quite negligible, since for all the measurements performed, the temperature of the joints was far enough from the glass transition temperature of the adhesive (see Table 2).

3.2. Fatigue tests

The results of the fatigue tests are given in terms of number of cycles to failure vs. average shear stress amplitude of the fatigue cycle in Figs. 11–18, while the coefficients of the best fit power equations (according to eq. (6)), together with the coefficient of determination (R^2),

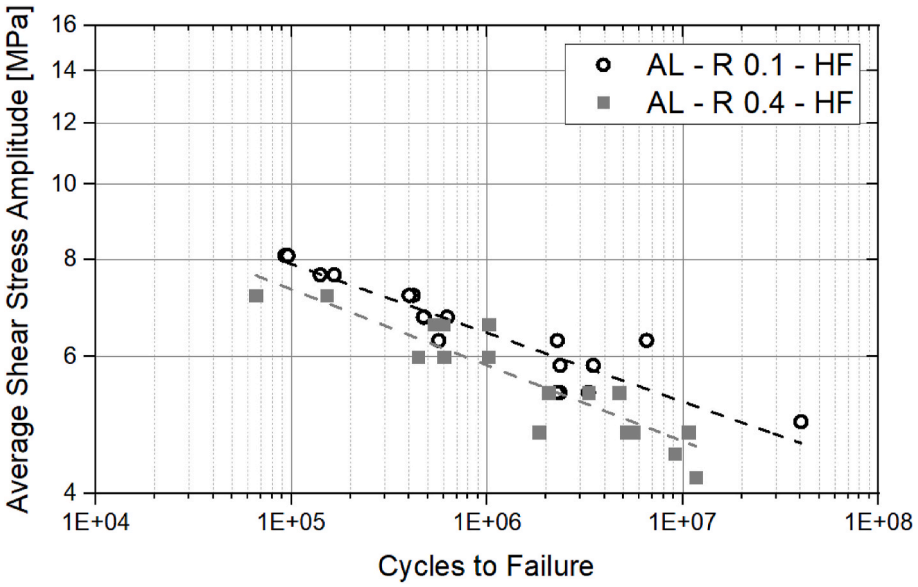

Fig. 16. Result of fatigue test, aluminum specimens, High Frequency.

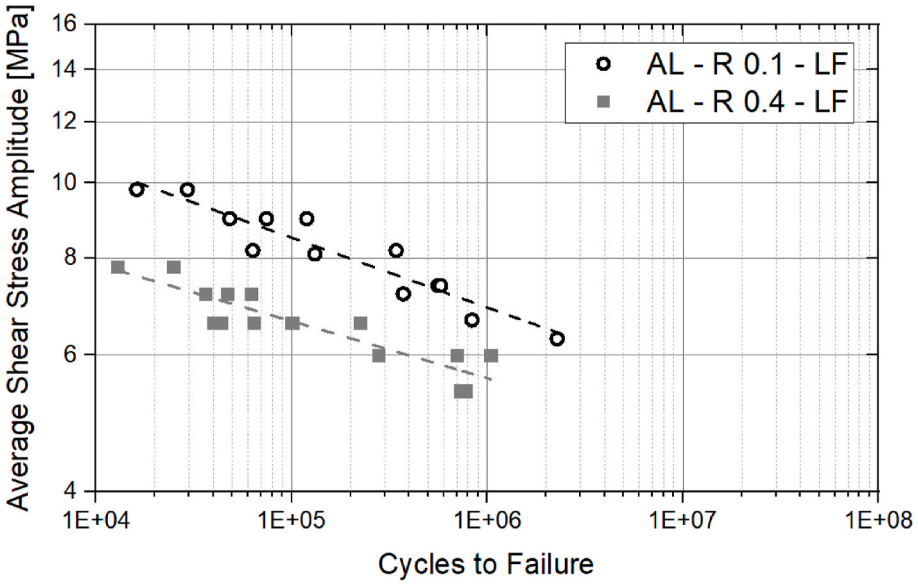

Fig. 17. Result of fatigue test, aluminum specimens, Low Frequency.

are given in Table 6 for every series of data. The first four graphs compare the fatigue behaviour of the joints considering the same material and load ratio, for the two different test frequencies. Figs. 12 and 14 show that the fatigue behaviour of both aluminum and stainless steel joints tested at R = 0.1 appeared to be only slightly affected by the frequency of the test: more in detail the two best fit curves of stainless steel joints tested at LF and HF are almost superimposed to each other. For the aluminum joints the two regression curves show almost the same slope (−0.088 for HF and −0.09 for LF), while they are slightly shifted in the vertical direction. Quite different comments can be drawn by looking at Figs. 13 and 15 where the fatigue behaviour for the two materials and load ratio equal to 0.4, is compared for the two loading frequencies. For the aluminum joints, the two sets of experimental data are rather close to each other, even though it appears that the slope of the HF best fit curve is quite higher than that of LF. This is in agreement with the result obtained in Ref. [20], and leads to a longer fatigue life of the HF joint for the higher loads, while for lower loads the two best fit curves become closer.

Considering the stainless steel joints, the slopes of both HF and LF best fit curves (−0.020 and −0.014 respectively) clearly appear much lower than in the previous cases (−0.06 and −0.097). Again, the frequency seems to slightly affect the results, since the two set of experimental points are close to each other and only small differences can be found in the slope of the best fit curves (the HF best fit curve results quite steeper compared to the LF one).

To better understand the results of the experimental campaign, the graphs given from Figs. 16–19 compare the experimental data for the same material and loading frequency, for the two different values of loading ratios. This kind of comparison is typically addressed to highlight the effect of the average load of the fatigue cycle.

Figs. 16 and 17 show the results obtained for the aluminum specimens. For the high frequency fatigue tests (Fig. 16), the two best fit curves corresponding to the load ratios R = 0.1 and R = 0.4 approximately present the same slope (−0.0885 and −0.0977, for R = 0.1 and R

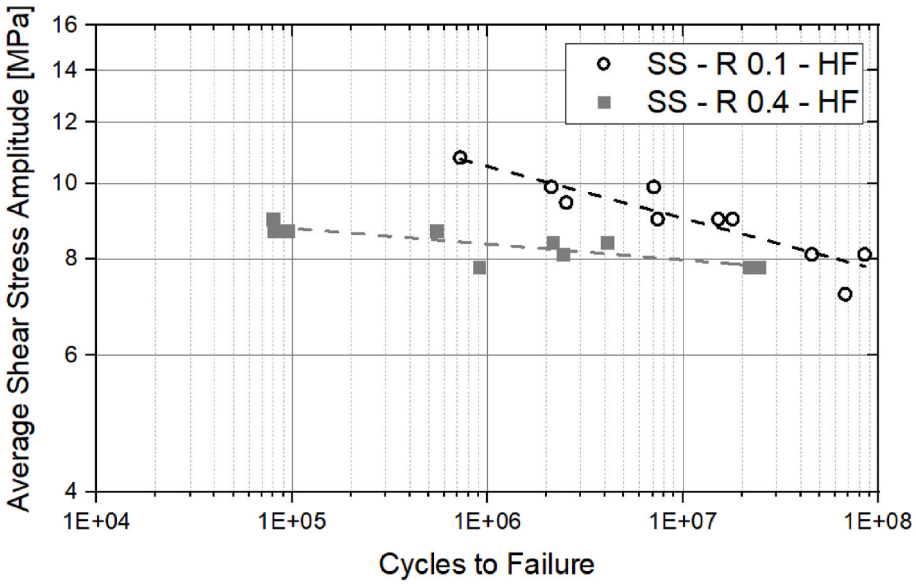

Fig. 18. Result of fatigue test, stainless steel specimens, High Frequency.

Table 6
Coefficients of the best fit equation (according to eq. (6)).

Group	k [MPa]	μ [ln MPa/ln cycles]	R^2
AL – HF – R = 0.1	21.89	−0.0885	0.854
AL – HF – R = 0.4	22.58	−0.0977	0.831
AL – LF – R = 0.1	23.97	−0.0900	0.878
AL – LF – R = 0.4	15.48	−0.0735	0.801
SS – HF – R = 0.1	26.48	−0.0668	0.832
SS – HF – R = 0.4	11.07	−0.0204	0.640
SS – LF – R = 0.1	30.02	−0.0739	0.921
SS – LF – R = 0.4	10.43	−0.0147	0.655

= 0.4 respectively), and the two sets of experimental points are quite close to each other. For the lowest load frequency (Fig. 17) it appears that the slope of the best fit curve of the tests carried out at R = 0.4 (−0.0735) is slightly lower than that associated with the tests carried out at R = 0.1 (−0.09), and, more noticeably, it appears that the two sets of data are completely separated. A first outcome of this comparison concerns the influence of the average load on the fatigue life of joints: the influence is rather limited when tests are carried out with the highest frequency, while it is emphasized when the fatigue testes are carried out at the lowest frequency.

The same comparison is given for stainless steel joints in Figs. 18 and 19. It clearly appears that the best fit curves of the experimental data resulted from fatigue tests carried out at R = 0.4 show slopes much lower than those obtained from test carried out at R = 0.1. Therefore, regardless of the loading frequency, for stainless steel joints, it can be stated that the average load plays a crucial role on the fatigue behaviour of bonded joints, and in particular the higher is the load ratio, the shorter will be the number of cycles at failure for a given shear stress amplitude τ_A.

The influence of the average load could be ascribed to some viscoelastic phenomena triggered in the adhesive layer. In general, creep effect in fatigue loading is related to the average load of the fatigue cycle [21]. Furthermore, it has to be considered that for a constant average

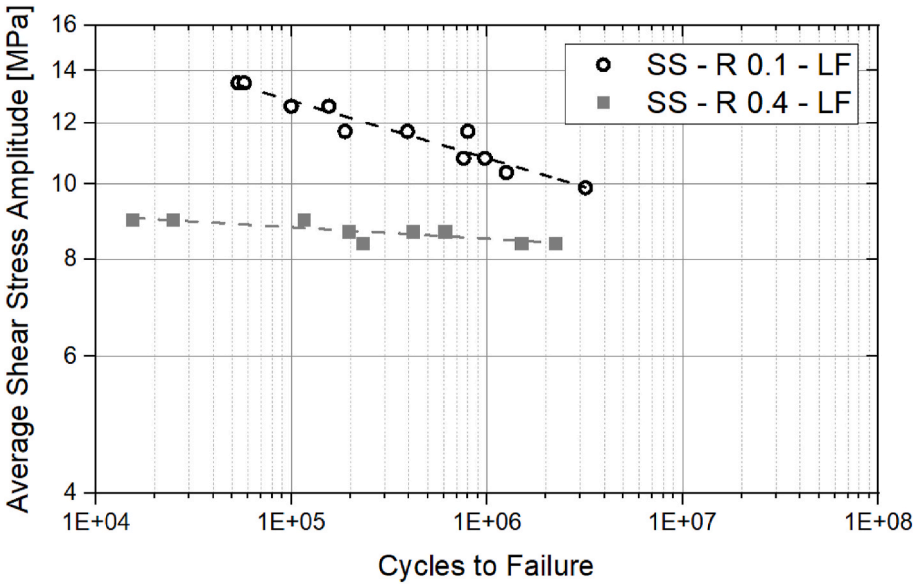

Fig. 19. Result of fatigue test, stainless steel specimens, Low Frequency.

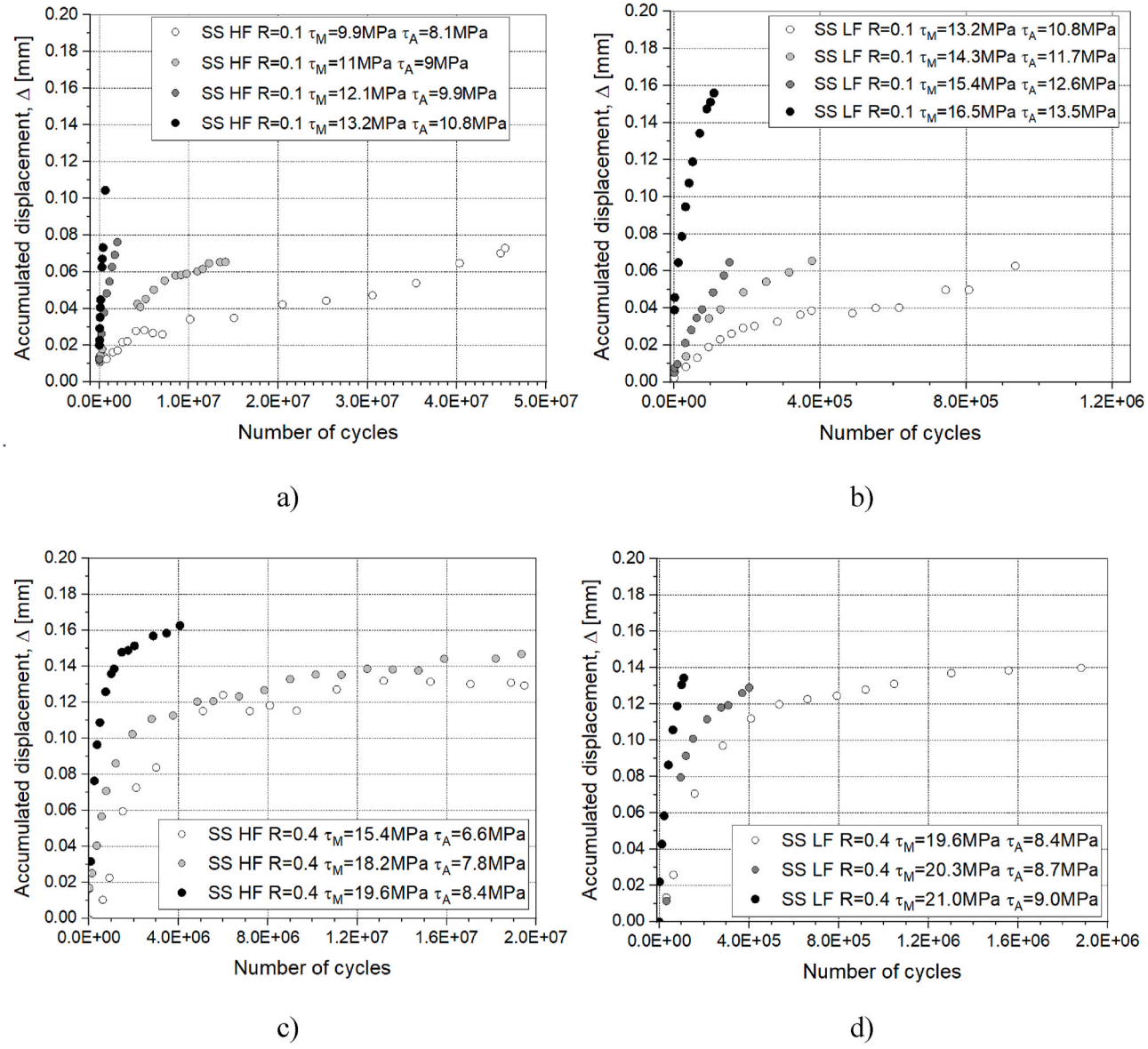

Fig. 20. Trend of accumulated displacement during the tests, stainless steel joints: a) High Frequency, Load Ratio 0.1, b) Low Frequency, Load Ratio 0.1, c) High Frequency, Load Ratio 0.4, d) Low Frequency, Load Ratio 0.4.

shear stress amplitude, the higher is the load ratio, the higher will be the average load. In addition, the load required to obtain the failure of the stainless steel joints in the considered range of number of cycles was higher (30–50 %) than that of aluminum joints (this is related to the smoother stress distribution of stainless steel joint due to the higher stiffness of the substrates). These considerations go exactly in the direction of experimental observation, and to better understand whether the fatigue tests were affected by viscoelastic phenomena, the amount of accumulated displacement (Δ) was monitored.

Figs. 20 and 21 show the trends of this measure under different testing conditions (material, test frequency and load ratio). From Fig. 20, it can be stated that a significant amount of accumulated displacement is found for the tests performed with the highest load ratio (c, d). It can be seen that Δ grows quickly at the beginning of the test; then the growth rate progressively decreases, until it reaches a sort of stable growth. Most of tests show a stable growth until final failure. For all stainless steel joints, tested with R = 0.4, the amount of accumulated displacement at failure reaches 0.14 ± 0.02 mm, that approximately corresponds to a 70 % of shear strain of the adhesive layer (the adhesive thickness was 0.2 mm). Moreover, it can be shown that the higher the load, the faster is the growth rate of the curves. The stainless steel joints tested at R = 0.1 (Fig. 20 a) and b)) show, in general, a smaller amount of accumulated displacement (most of the time less than 0.1 mm), with the only exception of specimens tested with the highest load at the lowest frequency, which shows a behavior quite similar to the previous one. However, the growth rate still depends on the magnitude of applied load.

Fig. 21 shows the same analysis for aluminum joints. Tests performed at the lowest load ratio show a small amount of accumulated displacement. Also the trend is quite different from that shown by stainless steel specimens, since Δ remains close to zero for most of the test and only begins to increase in the last part of the joint life. The final increase, likely, occurs when the propagation of defect in the adhesive layer leads to a reduction of the bearing section of the adhesive and therefore to an increase of the average shear stress, leading in turn to the onset of some viscoelastic phenomena. Tests carried out at R = 0.4 still show a significant amount of accumulated displacement, especially for test performed at lower frequencies. As already shown before, the lower the applied load, the slower is the growth rate of the accumulated displacement.

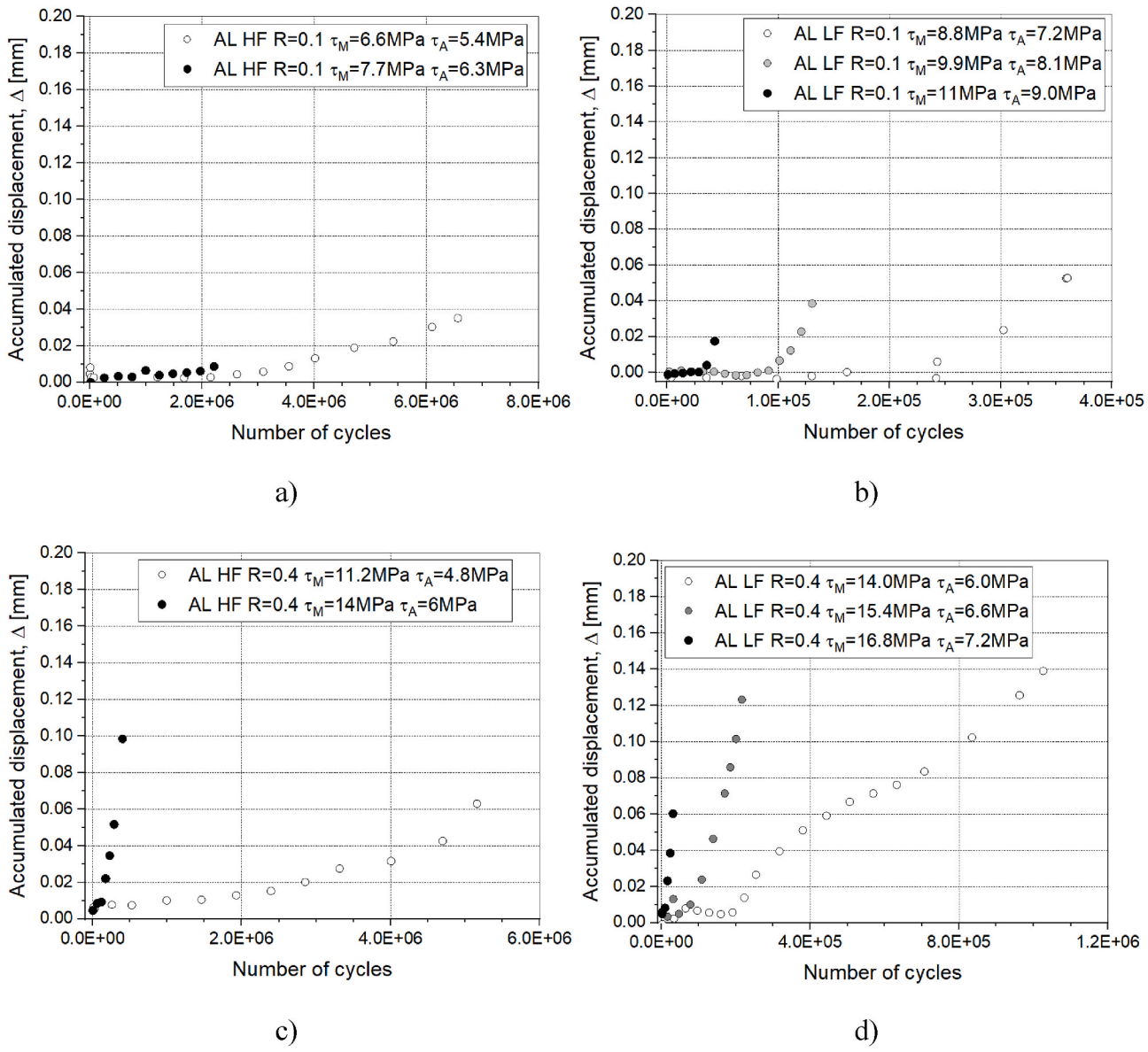

Fig. 21. Trend of accumulated displacement during the tests, aluminum joints: a) High Frequency, Load Ratio 0.1, b) Low Frequency, Load Ratio 0.1, c) High Frequency, Load Ratio 0.4, d) Low Frequency, Load Ratio 0.4.

As described in section 2.4, beyond the accumulated displacement (Δ), the joint stiffness (K) was also monitored during the test development. Tests that presented small amount of accumulated displacements showed a progressive reduction of joint stiffness during the test evolution (hollow circles in Fig. 22), leading to the conclusion that the fatigue progressively produced the onset and propagation of defects in the adhesive layer until the final fracture. On the opposite, for tests that presented a significant amount of accumulated displacement, the stiffness remained nearly constant for the entire life of the joints (grey circles in Fig. 22), leading to the conclusion that there was little or negligible reduction in the adhesive bearing area. In other words, the failure of the latter can be mainly ascribed to creep phenomena, rather than fatigue damage.

The study of stiffness variation during the test execution could, in principle, be another way to better discern the presence of significant viscoelastic phenomena during the fatigue tests. However, in this work, it did not allow to obtain straightforward results since, due to the experimental set up used, the stiffness measure presented a relatively high scatter with respect to the measure changes.

3.3. *Fracture surfaces*

Figs. 25, Figs. 24 and 23 show the comparison of fracture surface of some representative specimens: each figure compares the results of specimens tested at low and high frequency, with the same load ratio, and similar applied loads. In general, it can be seen that for every material, load ratio and test frequency considered, the fracture surfaces presented a mixed failure. Most of time the cracks were generated on both side of the overlap, in the proximity of the interface with the substrates (Fig. 26).

Typically, the cracks propagated for few millimetres until the reduction of the residual bond lead to the quasi static failure of the joins. This kind of final failure was identified by the presence of extensive whitening of the adhesive in the central parte of the overlap. The presence of whitening is more pronounced for the stainless steel joints, since they presented higher applied loads (to exhibit the same number of cycles at failure of Aluminum joints).

In conclusion it can be stated that the fracture surfaces were not significantly affected by the test frequency.

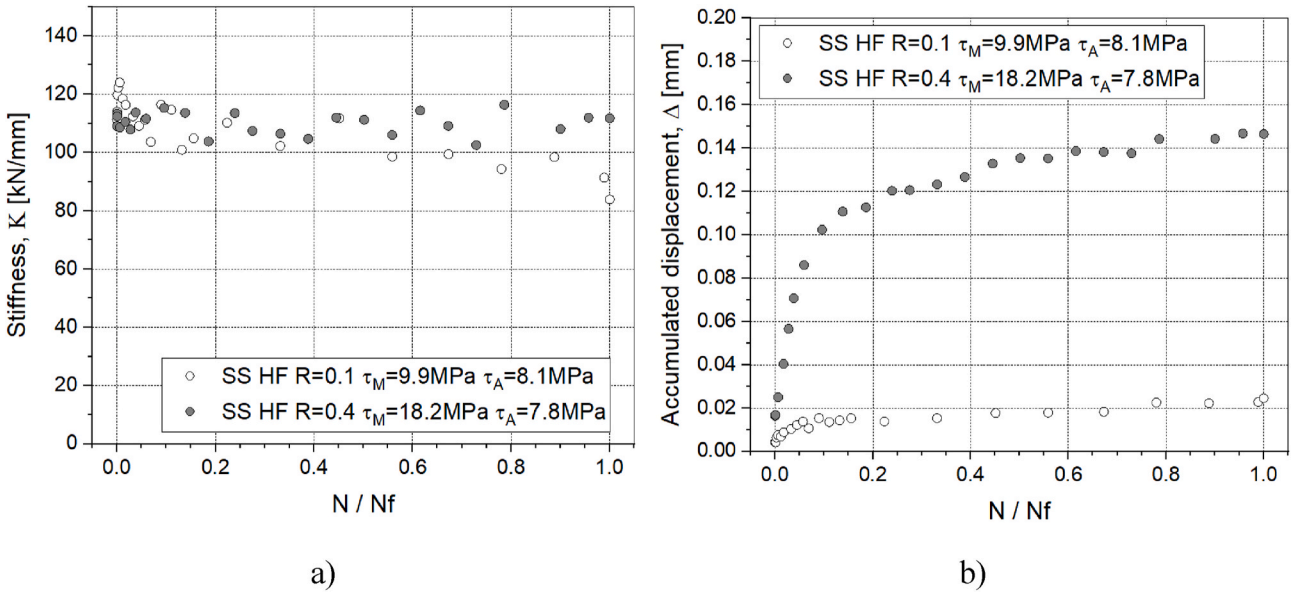

Fig. 22. Example of trend of a) joints stiffness and b) accumulated displacement during tests with significant (SS HF R = 0.4 τ_M = 18.2 MPa τ_A = 7.87 MPa) and negligible (SS HF R = 0.1 τ_M = 9.9 MPa τ_A = 8.1 MPa) accumulated displacement, as a function of normalized number of cycles.

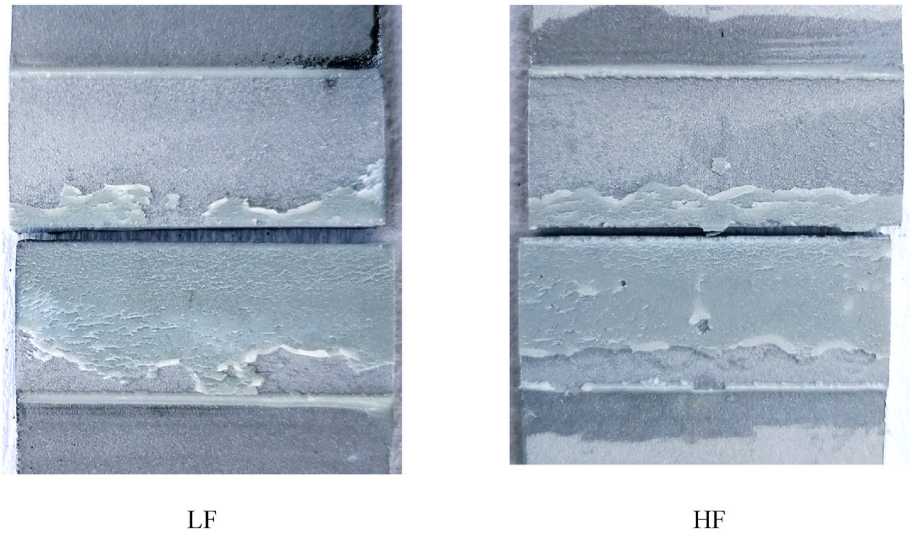

Fig. 23. Example of fracture surfaces for AL joints, load ratio R = 0.1.

3.4. Discussion

Generally speaking, the results of this work seem in agreement with some findings in literature. The insensitivity of the fatigue behavior to the selected value of cycle frequency was reported in Ref. [29], for epoxy adhesive systems and limited to a frequency range of 0.5–5 Hz which however presents differences of one order of magnitude between extreme values. In Ref. [30] the insensitivity of the fatigue life to the frequency, in the range 2–10 Hz, was justified in light of the neglectable increase of temperature associated to higher frequencies (as in the present case) which made the adhesive being tested, regardless of the frequency, in its glassy domain where limited rate effects were expected. In the same paper, the mean load was identified to have a deleterious effect on the fatigue life of joints and, in Ref. [22], the hold time at maximum load was found to strongly affect the fatigue life while the hold time at minimum load had not any consequences on the durability of joints, resulting in a correlation between the occurrence of creep events and the value of the load ratio, as highlighted also in Ref. [30]. The role of the load ratio in increasing the crack growth rate in Double Cantilever Beam (DCB) joints bonded with specific adhesive systems (e.g.: epoxy, PMMA) was reported also in Ref. [31], where it was directly related to a high creep crack extension, which could also be applied to other similar cases where the same adhesive systems were adopted [32]. Even in Ref. [33] the load ratio and the mean load were reported to influence the fatigue life to a higher degree than the loading cycle frequency. However, the association usually performed in literature between creep and low frequency loading cycles ([18,34,35]) could lead to the general misleading conclusion, as stated in Ref. [18], that high frequency test data should not be used to predict the fatigue life of joints which used to undergo low frequency loading cycles. This is certainly true when the applied maximum load overcomes a threshold capable to trigger viscoelastic phenomena, but lower loads result in a low sensitivity to the frequency used for cyclically loading the joints: for instance, in Ref. [30] a graph displays the trend of the normalized load range for T-peel joints vs. the number of cycles to failure for two different values of frequency (2 and 10 Hz, respectively) from which any significant

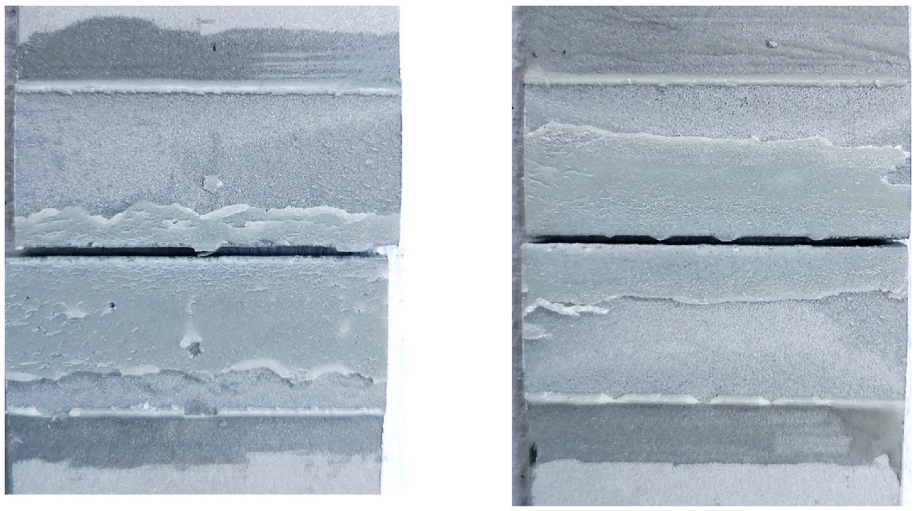

Fig. 24. Example of fracture surfaces for AL joints, load ratio R = 0.4.

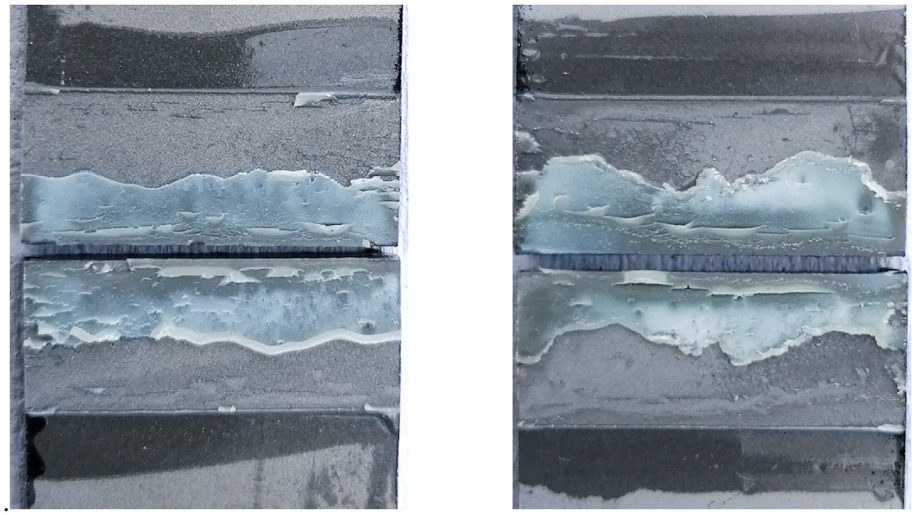

Fig. 25. Example of fracture surfaces for SS joints, load ratio R = 0.4.

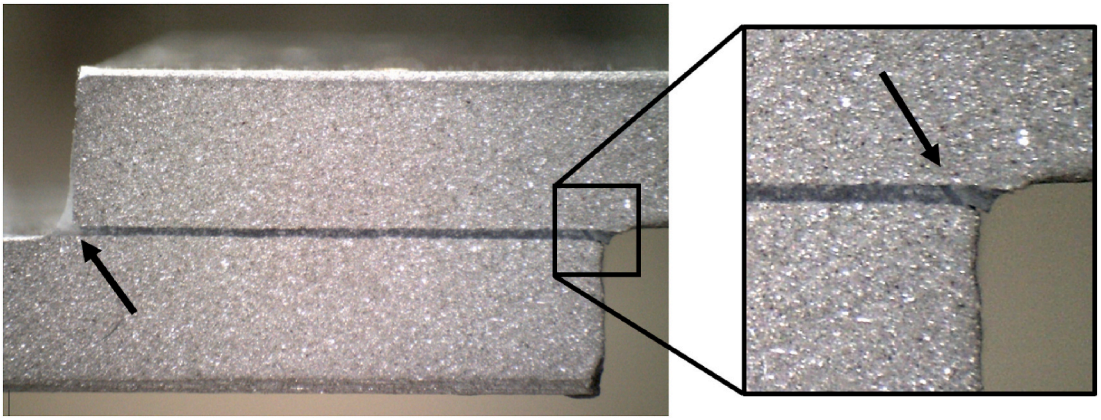

Fig. 26. Crack onset on both ends of the overlap.

difference related to frequency could be found for normalized load ranges lower than about 0.65. In the case of present work, the ratio between the minimum average shear stress induced of the cycle, $\tau_{MIN} = \tau_M - \tau_A$, and the quasi static average shear strength, τ_{ADH}, identified in Ref. [36] for the same kind of specimens used for the present work, could be exploited to identify a range of values which segregate the cases in which creep events become prevalent with respect to the evolution of fatigue damage (resulting in a lower fatigue life for low frequency cycles) from the cases in which the creep phenomena are less relevant and do not affect the sensitivity of the fatigue behavior to the frequency. In particular, for aluminum joints, the accumulated displacement during a fatigue test starts becoming relevant when τ_{MIN}/τ_{ADH} is approximately equal to 15–20 %, while for stainless steel joints the critical value of the ratio is around 5–10 %. In conclusion, the effectiveness of high frequency tests in speeding-up the fatigue characterization for the ranges of cycles to failure usually explored by standard testing and in investigating the behavior for ranges of cycles to failure usually unexplored due to the high time cost they would require is here demonstrated, but it must be properly limited to cases in which the minimum load of the applied cycle does not overcome a specific rate of the static strength of the joints, depending on their materials and dimensions.

4. Conclusion

In this work, the influence of the test frequency on the fatigue behaviour of metal-epoxy bonded joints was investigated, for two substrate materials and two load ratios. In particular, the comparison was done between frequencies between 7 and 9 Hz (LF) and 70–90 Hz (HF). Preliminary investigations, consisting in DMA and temperature measurement of the adhesive layer during HF fatigue tests, revealed that a negligible heating was generated due to hysteretic phenomena, since the dynamic behaviour of the adhesive remained mainly elastic. The results of the fatigue experimental campaign clearly indicated that high frequency fatigue testing could be an effective way to shorten time of testing for bonded joints, even though only under certain conditions. In particular, good agreement was found between the LF and HF fatigue behaviour when the loading conditions did not trigger viscoelastic phenomena, therefore for low load ratios and low applied loads. For higher load ratios, and also for low load ratios but high applied loads, the presence of creep phenomena was clearly identified, and under this condition the agreement between the experimental results of LF and HF fatigue testing was lost. In conclusion, high frequency fatigue testing is suitable for investigating the mechanical behaviour of metal bonded joints, and allows to characterize their fatigue behaviour at a number of cycles one or two order of magnitude higher than the one explored by the most of the literature works.

Funding

This research did not receive any specific grant from funding agencies in the public, commercial, or not-for-profit sectors.

Declaration of competing interest

The authors declare that they have no known competing financial interests or personal relationships that could have appeared to influence the work reported in this paper.

Data availability

Data will be made available on request.

References

[1] Abdel Wahab MM. Fatigue in adhesively bonded joints: a review. ISRN Mat. Sci. 2021. https://doi.org/10.5402/2012/746308. Article ID 746308.
[2] Sousa FC, Akhavan-Safar A, Carbas RJC, Marques EAS, Barbosa AQ, da Silva LFM. Int J Fatig 2023;175:107752. https://doi.org/10.1016/j.ijfatigue.2023.107752.
[3] Santos D, Akhavan-Safar A, Carbas RJC, Marques EAS, Wenig S, da Silva LFM. Load-control vs. displacement-control strategy in fatigue threshold analysis of adhesives: effects of temperature. Eng Fract Mech 2023;284:109255. https://doi.org/10.1016/j.engfracmech.2023.109255.
[4] Arakawa J, Jinnouchi W, Akebono H, Sugeta A. Effect of pre-water immersion period on fatigue resistance of adhesive bonded thin steel. Int J Fatig 2023;174:107725. https://doi.org/10.1016/j.ijfatigue.2023.107725.
[5] Wang S, Fan J, Li H, Wang H, Lan Z, Liu J, Peng J, Zhu M. Fatigue failure analysis of CFRP single-lap adhesive-riveted hybrid joints. Tribol Int 2023;188:108854. https://doi.org/10.1016/j.triboint.2023.108854.
[6] Zhang X, Ju Y, Zhu A, Zou T. Fatigue beahvior of single-lap adhesive joints with similar and dissimilar adherends under cyclic loading: a combined experimental and simulation study. Mater Today Commun 2023;37:107215. https://doi.org/10.1016/j.mtcomm.2023.107215.
[7] He Z, Luo Q, Li Q, Zheng G, Sun G. Fatigue behavior of CFRP/Al adhesive joints – failure mechanisms study using digital image correlation (DIC) technique. Thin-Walled Struct 2022;174:109075. https://doi.org/10.1016/j.tws.2022.109075.
[8] Bali G, Topkaya T. Effect of graphene nano-particle reinforcement on the fatigue behavior of adhesively bonded single lap joints. Int J Adhesion Adhes 2023;120:103279. https://doi.org/10.1016/j.ijadhadh.2022.103279.
[9] Eghbalpoor R, Akhavan-Safar A, Jalali S, Ayatollahi MR, da Silva LFM. A progressive damage model to predict the shear and mixed-mode low-cycle impact fatigue life of adhesive joints using cohesive elements. Finite Elem Anal Des 2023;216:103894. https://doi.org/10.1016/j.finel.2022.103894.
[10] Geng F, Suiker ASJ, Rezaeiha A, Montazeri H, Blocken B. A computational framework for the lifetime prediction of vertical-axis wind turbines: CFD simulations and high-cycle fatigue modeling. Int J Solid Struct 2023;284:112504. https://doi.org/10.1016/j.ijsolstr.2023.112504.
[11] Khoshmanesh S, Watson SJ, Zarouchas D. The effect of the fatigue damage accumulation process on the damping and stiffness properties of adhesively bonded composite structures. Compos Struct 2022;287:115328. https://doi.org/10.1016/j.compstruct.2022.115328.
[12] Sun Q, Sun Z, Zhu H, Lu Y. An electrical-mechanical cohesive zone model combining viscoelasticity and fatigue damage for soft adhesive layer in wearable sensor. Eng Fract Mech 2022;276:108897. https://doi.org/10.1016/j.engfracmech.2022.108897.
[13] Nejad RM, Moghadam DG, Hadi M, Zamani P, Berto F. An investigation on static and fatigue life evaluation of grooved adhesively bonded T-joints. Structures 2022;35:340–9. https://doi.org/10.1016/j.istruc.2021.11.025.
[14] Jeandrau JP, Peyrac C, Lefebvre F, Renard J, Gantchenko V, Patamaprohm B, Guinault C. Fatigue behaviour of adhesive joints. Procedia Eng 2015;133:508–17. https://doi.org/10.1016/j.proeng.2015.12.622.
[15] Trapezon OG. Experimental procedure for the in-shear adhesive strength evaluation under high-frequency cyclic loading. Strength Mater 2021;53:751–8. https://doi.org/10.1007/s11223-021-00340-9.
[16] Takamizawa T, Scheidel DD, Barkmeier WW, Erickson RL, Tsujimoto A, Latta MA, Miyazaki M. Influence of frequency on shear fatigue strength of resin composite to enamel bonds using self-etch adhesives. J Mech Behav Biomed Mater 2016;62:291–8. https://doi.org/10.1016/j.jmbbm.2016.05.017.
[17] Xu X, Crocombe AD, Smith PA. Fatigue crack growth rates in adhesive joints tested at different frequencies. J Adhes 1996;58:191–204. https://doi.org/10.1080/00218469608015200.
[18] Al-Ghamdi AH, Ashcroft IA, Crocombe AD, Abdel-Wahab MM. Crack growth in adhesively bonded joints subjected to variable frequency fatigue loading. J Adhes 2003;79:1161. https://doi.org/10.1080/714906165.
[19] Erpolat S, Ashcroft IA, Crocombe AD, Abdel-Wahab MM. A study of adhesively bonded joints subjected to constant and variable amplitude fatigue. Int J Fatig 2004;26:1189–96. https://doi.org/10.1016/j.ijfatigue.2004.03.011.
[20] Perruchoud V, Vassilopoulos AP. The challenges of quasi-static and fatigue experiments of structural adhesives. Int J Fatig 2022;162:106980. https://doi.org/10.1016/j.ijfatigue.2022.106980.
[21] Gomatam RR, Sancaktar E. The effects of stress state, loading frequency and cyclic waveforms on the fatigue behavior of silver-filled electronically-conductive adhesive joints. J Adhes Sci Technol 2006;20:53–68. https://doi.org/10.1163/156856106775212378.
[22] Tridello A, Ciardiello R, Paolino DS, Goglio L. Fatigue response up to 10^9 cycles of a structural epoxy adhesive. Fatig Fract Eng Mater Struct 2020:1–12. https://doi.org/10.1111/ffe.13240.
[23] Veer FA, Schönwälder J, Zuidema J, van Kranenburg C. Failure criteria for transparent acrylic adhesive joints under static, fatigue and creep loading. In: Proceedings of the 15th European conference on fracture – ECF, vol. 15. Stockolm; 2004.
[24] ASTM D 3166 - 99. Standard test method for fatigue properties of adhesives in shear by tension loading (Metal/Metal). West Conshohocken: ASTM International; 2020.
[25] ISO 25178-2:2012 Geometrical product specifications (GPS). Surface texture: areal – Part 2: terms, definitions and surface texture parameters. Geneva: International Organization for Standardization; 2012.
[26] Moroni F. Fatigue behaviour of hybrid clinch-bonded and self-piercing rivet bonded joints. J Adhes 2019;95:577–94. https://doi.org/10.1080/00218464.2018.1552586.
[27] Turner DZ. Digital image correlation engine (DICe) reference manual, sandia report, SAND2015-10606 O. 2015. Available online: https://www.osti.gov/biblio/1245432-digital-image-correlation-engine. [Accessed 20 February 2021].

[28] Ahrens James, Geveci Berk, Law Charles. ParaView: an end-user tool for large data visualization, visualization handbook. ISBN-13: 9780123875822. Elsevier; 2005.
[29] Luckyram J, Vardy AE. Fatigue performance of two structural adhesives. J Adhes 1998;26:273–91.
[30] Crocombe AD, Richardson G. Assessing stress state and mean load effects on the fatigue response of adhesively bonded joints. Int J Adhesion Adhes 1999;19:19–27.
[31] Hertzberg RW, Manson JA. Fatigue of engineering plastics. New York and London: Academic Press, Inc.; 1980.
[32] Pirondi A, Nicoletto G. Fatigue crack growth in bonded DCB specimens. Eng Fract Mech 2002;71:859–71. https://doi.org/10.1016/S0013-7944(03)00046-8.
[33] Sawada, T., Fatigue fracture criteria in single-lap adhesive joints with cumulative dissipated energy.
[34] Zeng Q, Sun CT. Fatigue performance of a bonded wavy composite lap joint. Fatig Fract Eng Mater Struct 2003;27:413–22. https://doi.org/10.1111/j.1460-2695.2004.00761.x.
[35] Gladkov A, Bar-Cohen A. Parametric dependence of fatigue on electronic adhesives. IEEE Trans Compon Packag Manuf Technol 1999;22(2):200–8.
[36] Moroni F, Musiari F, Favi C. Effect of the surface morphology over the fatigue performance of metallic single lap-shear joints. Int J Adhesion Adhes 2020;97:102484. https://doi.org/10.1016/j.ijadhadh.2019.102484.